


Functional dissection of *HGGT* and *HPT* in barley vitamin E biosynthesis via CRISPR/Cas9-enabled genome editing

Zhanghui Zeng^{1,†}, Ning Han^{1,†}, Cuicui Liu¹, B. Buerte¹, Chenlu Zhou¹, Jianshu Chen², Mengyao Wang¹, Yuhong Zhang³, Yawei Tang³, Muyuan Zhu¹, Junhui Wang¹, Yinong Yang⁴ and Hongwu Bian^{1,*} 

¹Institute of Genetics and Regenerative Biology, Key Laboratory for Cell and Gene Engineering of Zhejiang Province, College of Life Sciences, Zhejiang University, Hangzhou, 310058, China, ²College of Pharmaceutical Science, Zhejiang University of Technology, Hangzhou, 310014, China, ³Tibet Academy of Agricultural and Animal Husbandry Sciences, Lhasa, 850000, China and ⁴Department of Plant Pathology and Environment Microbiology, The Huck Institutes of the Life Sciences, The Pennsylvania State University, University Park, PA, 16802, USA

* For correspondence. E-mail hwbian@zju.edu.cn

† These authors contributed equally to this work.

Received: 16 March 2020 Returned for revision: 22 April 2020 Editorial decision: 10 June 2020 Accepted: 18 June 2020
Electronically published: 24 June 2020

- **Background and Aims** Vitamin E (tocochromanol) is a lipid-soluble antioxidant and an essential nutrient for human health. Among cereal crops, barley (*Hordeum vulgare*) contains a high level of vitamin E, which includes both tocopherols and tocotrienols. Although the vitamin E biosynthetic pathway has been characterized in dicots, such as *Arabidopsis*, which only accumulate tocopherols, knowledge regarding vitamin E biosynthesis in monocots is limited because of the lack of functional mutants. This study aimed to obtain gene knockout mutants to elucidate the genetic control of vitamin E composition in barley.
- **Methods** Targeted knockout mutations of *HvHPT* and *HvHGGT* in barley were created with CRISPR/Cas9-enabled genome editing. High-performance liquid chromatography (HPLC) was performed to analyse the content of tocochromanol isomers in transgene-free homozygous *Hvhpt* and *Hvhggt* mutants.
- **Key Results** Mutagenesis efficiency among T₀ regenerated plantlets was 50–65 % as a result of two simultaneously expressed guide RNAs targeting each gene; most of the mutations were stably inherited by the next generation. The transgene-free homozygous mutants of *Hvhpt* and *Hvhggt* exhibited decreased grain size and weight, and the *HvHGGT* mutation led to a shrunken phenotype and significantly lower total starch content in grains. HPLC analysis revealed that targeted mutation of *HvHPT* significantly reduced the content of both tocopherols and tocotrienols, whereas mutations in *HvHGGT* completely blocked tocotrienol biosynthesis in barley grains. Transient overexpression of an *HvHPT* homologue in tobacco leaves significantly increased the production of γ - and δ -tocopherols, which may partly explain why targeted mutation of *HvHPT* in barley grains did not eliminate tocopherol production.
- **Conclusions** Our results functionally validated that *HvHGGT* is the only committed gene for the production of tocotrienols, whereas *HvHPT* is partly responsible for tocopherol biosynthesis in barley.

Key words: Barley (*Hordeum vulgare*), CRISPR/Cas9, *HvHGGT*, *HvHPT*, genome editing, tocopherol, tocotrienol, vitamin E.

INTRODUCTION

Vitamin E (tocochromanol) is a potent lipid-soluble antioxidant and an essential component of the human diet. Many human diseases, such as cardiovascular disease and certain cancers, are associated with insufficient vitamin E intake (Bramley *et al.*, 2000). Because of its beneficial effect, the daily requirement of vitamin E for humans has been raised to 15–30 mg (DellaPenna, 2005). To meet the demand for human consumption, it is necessary to modify the level and composition of vitamin E in food crops via genome engineering and precision plant breeding.

Vitamin E is classified into two categories, tocopherols (T) and tocotrienols (T3), both of which contain a polar chromanol head group linked to an isoprenoid (phytyl) side chain. There are four T forms (α -T, β -T, γ -T and δ -T) and four T3 forms (α -T3, β -T3, γ -T3 and δ -T3), which are based on the number

and position of methyl groups on the chromanol head group (Schneider, 2005; Falk and Munne-Bosch, 2010). Tocopherols and tocotrienols differ in their degree of unsaturation: tocopherols have a fully saturated phytyl tail arising from the C20 isoprenoid intermediate phytyl diphosphate (PDP); tocotrienols have an unsaturated side chain with three *trans* double bonds that is derived from the C20 isoprenoid intermediate geranylgeranyl diphosphate (GGDP). Although tocopherol and tocotrienol both function as potent antioxidants, they exhibit distinctive biological properties. Tocopherols, typically in the α form, are widely distributed in photosynthetic plants, whereas tocotrienols occur primarily in the seed endosperm of most monocots and a limited number of dicots (Horvath *et al.*, 2006; Falk and Munne-Bosch, 2010; Yang *et al.*, 2011). *In vitro* studies indicate that α -tocopherol is the most active

form of vitamin E, interacting with the polyunsaturated acyl groups of lipids, stabilizing membranes, and scavenging and quenching various reactive oxygen species. Therefore, tocopherols play an important role in protecting oxygenic phototrophs from lipid peroxidation (Maeda *et al.*, 2005). However, in some cases, tocotrienols possess superior biological properties to tocopherols, including hypocholesterolaemic, anticancer and neuroprotective activities, which are not often observed in tocopherols (Sen *et al.*, 2007; Aggarwal *et al.*, 2010; Chin *et al.*, 2016).

Tocopherols and tocotrienols are synthesized in plastids of plant cells (Yang *et al.*, 2011; Lushchak and Semchuk, 2012) and their biosynthetic pathways have been elucidated (Schneider, 2005; Chen *et al.*, 2006). Following the synthesis of tyrosine and its derivative 4-hydroxyphenylpyruvate (HPP) via the shikimate pathway, *p*-hydroxyphenylpyruvate dioxygenase catalyses the conversion of HPP to homogentisate (HGA). The committed step in tocopherol biosynthesis has traditionally been considered the condensation of HGA and PDP to form 2-methyl-6-phytyl-1,4-benzoquinol (MPBQ), as catalysed by homogentisate phytyltransferase (HPT). Tocotrienol biosynthesis involves GGDP rather than PDP, which is different from that of tocopherol synthesis. GGDP is directly condensed with HGA by homogentisate geranylgeranyl transferase (HGGT), producing 2-methyl-6-geranylgeranyl-1,4-benzoquinol (MGGBQ). In tocopherol and chlorophyll biosynthesis, GGDP reductase carries out the conversion of GGDP to PDP (Keller *et al.*, 1998). Subsequent reactions in tocotrienol and tocopherol syntheses are similar, including ring methylations and ring cyclization, which are catalysed by the common enzymes 2-methyl-6-phytylbenzoquinone methyltransferase, tocopherol cyclase and γ -tocopherol methyltransferase (γ -TMT).

HGGT and HPT, two committed enzymes in the vitamin E biosynthesis pathway, are the main targets for metabolic engineering of both tocopherols and tocotrienols in plants. In dicots, such as *Arabidopsis*, the vitamin E biosynthesis pathway has been well established (Collakova and DellaPenna, 2003; Sattler *et al.*, 2004; Gilliland *et al.*, 2006; Valentin *et al.*, 2006). Deletion in the *HPT* (*VTE2*) gene results in total tocopherol deficiency in all tissues (Sattler *et al.*, 2004), whereas overexpression of *Arabidopsis HPT* (*HPT1*) causes a 4.4-fold increase in total tocopherol levels in leaves compared to that in the wild-type (Collakova and DellaPenna, 2003). Furthermore, the content of α -tocopherol has been increased by co-overexpression of *HPT1* and the gene encoding γ -TMT, resulting in a 12-fold increase in vitamin E activity. However, only modest increases in vitamin E contents in the seeds of soybeans (*Glycine max*) and *Arabidopsis* occurred by enhancing the expression of *HPT* (Savidge *et al.*, 2002; Collakova and DellaPenna, 2003; Karunanandaa *et al.*, 2005). *HGGT*, which probably evolved in monocots, is predicted to be functionally divergent from *HPT*, which is conserved in both monocot and dicot species (Cahoon *et al.*, 2003). Overexpression of barley *HGGT* in *Arabidopsis*, soybeans and tobacco results in considerable accumulation of total vitamin E, primarily in the form of tocotrienols (Cahoon *et al.*, 2003; Konda *et al.*, 2020), although expression of rice *HGGT* in soybeans only led to a slight accumulation of tocotrienols (Kim *et al.*, 2011). Our recent work has demonstrated that overexpression of *HvHGGT* can significantly enhance tocotrienol levels and antioxidant activities while altering

the composition of vitamin E in transgenic barley grains (Chen *et al.*, 2017). Moreover, a recent joint linkage and genome-wide association study in 5000 lines of US maize (*Zea mays*) showed that allelic variation in 14 genes is responsible for 56–93 % of tocochromanol production in grains (Diepenbrock *et al.*, 2017). In hexaploid oat (*Avena sativa*), two of five *HPT* (*VTE2*) homologues were identified as highly correlated with tocochromanol accumulation through deep sequencing and orthology-guided assembly (Gutierrez-Gonzalez and Garvin, 2016). Surprisingly, among the three *HGGT* homologues, one did not correlate with tocochromanol content, whereas the others had negative correlation coefficients (Gutierrez-Gonzalez and Garvin, 2016). Although transgenic overexpression of *HPT* or *HGGT* has been conducted to increase vitamin E content or alter the composition of vitamin E in monocot plants, the lack of functional mutants in the main step of the vitamin E pathway has impeded our understanding of tocochromanol biosynthesis in agronomically important cereal crops.

Barley (*Hordeum vulgare*), the fourth most important cereal crop in the world, is an excellent source of biologically active nutrients, including dietary fibre, β -glucans, phenolic acids, sterols, tocopherols and tocotrienols (Andersson *et al.*, 2008; Cai *et al.*, 2016). Barley and oats contain higher levels of tocochromanols compared with other cereals (Gutierrez-Gonzalez and Garvin, 2016). In particular, barley contains eight naturally occurring isomers of tocochromanol, and thus serves as a valuable source of vitamin E and an appropriate crop plant for genetic manipulation of vitamin E levels and composition. Despite the aforementioned progress in studying vitamin E biosynthesis in plants, there are few reports on metabolic engineering of tocopherol and tocotrienol biosynthesis in barley, which is partly because of the low efficiency of barley transformation and the lack of effective genome engineering tools. Recently, the CRISPR/CRISPR-associated protein 9 nuclease (Cas9) system has emerged as an efficient and versatile tool for genome editing and precision plant breeding (Xie *et al.*, 2015; Shen *et al.*, 2018; Cui *et al.*, 2020).

In the present study, barley *HvHGGT* and *HvHPT* mutants were successfully created with CRISPR/Cas9-enabled genome editing for genetic and developmental analyses. Phenotypic analysis of grains showed that the transgene-free homozygous *Hvhpt* and *Hvhggt* mutants had decreased grain size and total starch content. Analysis of vitamin E components revealed that *HvHGGT* was the only committed gene that produced tocotrienols, whereas *HvHPT* was not the only gene that controls the synthesis of tocopherols in barley.

MATERIALS AND METHODS

gRNA design and vector construction

Gene sequences of barley *HvHPT* (*HORVU7Hr1G110990*) and *HvHGGT* (*HORVU7Hr1G114330*) were downloaded from Ensembl Plants (http://plants.ensembl.org/Hordeum_vulgare/Info/Index). Based on these sequences, four single guide RNAs (gRNAs) were designed and synthesized for targeting four distinct protospacer regions using the web tool CRISPR-P (<http://cbi.hzau.edu.cn/crispr/>) (Lei *et al.*, 2014). Editing constructs containing the tRNA–gRNA fragment

were generated according to the method of Xie *et al.* (2015). The pGTR plasmid was used as a template to amplify the gRNA–tRNA fusion. pRGEB32, a binary vector, carries an *hpt* selection marker and a cloning site for insertion of the gRNA–tRNA fragment. Two tRNA–gRNA fragments were individually cloned into pRGEB32, resulting in two editing constructs: *PTG-HPT/Cas9* (gRNA1 + gRNA2) and *PTG-HGGT/Cas9* (gRNA3 + gRNA4) (the primers used for the DNA constructs are listed in [Supplementary Data Table S1](#) and detailed sequences of the two PTG constructs are provided in [Table S2](#)). These constructs were sequenced to ensure the accuracy of each tRNA–gRNA insert before they were electroporated into *Agrobacterium tumefaciens* strain EHA105 for barley transformation.

Plant material and genetic transformation

Wild-type spring barley plants (*H. vulgare* L. ‘Golden Promise’), obtained from the Australian Centre for Plant Functional Genomics at the University of Adelaide, were grown from October to April in experimental fields under natural conditions at the Agricultural Experiment Station of Zhejiang University, Hangzhou, Zhejiang Province, China. Caryopses were harvested 2–3 weeks after pollination. The immature scutella, 1.5–2 mm in size, were obtained from barley embryos after removal of the embryo axis and used as explants for *Agrobacterium*-mediated transformation following the procedure of Harwood (2014). Transgenic calli were induced from infected immature scutella on hygromycin (50 mg L⁻¹) containing medium, and plantlets resistant to hygromycin were regenerated. Regenerated plants at the seedling stage were grown for 12–16 weeks in a growth chamber with a 16-h light/8-h night cycle, a temperature of 23 °C and 70 % humidity. Subsequently, transgenic plants were grown until maturity under natural light in 6-inch pots in a glasshouse.

Molecular characterization of transgenic plants

Genomic DNA was extracted from leaves sampled from putative transgenic regenerants ~4 months after genetic transformation; at this stage, plantlets are 8–15 cm high. To identify transgenic lines, T₀ regenerated plantlets were first screened for the presence of the gRNA/Cas9 transgene using the primer pair pU3-Forward (5′-TGGGTACGTTGGAAACCACG-3′) and pUBI10-Reverse (5′-GTTTGTGGTCGCCGT TAGG-3′). PCR was carried out using Taq DNA polymerase (Vazyme Biotech, Jiangsu, China) with an XP thermal cycler (Bioer Technology, Hangzhou, China). The cycling conditions comprised an initial denaturation step at 95 °C for 5 min, followed by 32 cycles of 95 °C for 30 s, 60 °C for 30 s, 72 °C for 1 min, and a final extension step at 72 °C for 8 min. The product was analysed by 1.5 % (w/v) agarose gel electrophoresis. To detect mutagenesis at gRNA target sites, DNA samples positive for gRNA/Cas9 fragments were again assessed by mutation genotyping using specific primers ([Supplementary Data Table S3](#)). The PCR product was examined by 2 % agarose gel electrophoresis and stained with ethidium bromide to detect chromosomal-fragment deletions. To detect indels at desired

sites, the PCR product was further separated by 14 % SDS-PAGE (sodium dodecyl sulphate–polyacrylamide gel electrophoresis). Selected PCR products were sequenced directly by Shanghai Boshang Biology Company (Shanghai, China) or purified using a DNA Purification Kit (Sangon Biotech, Shanghai, China) and then transferred into the pClone007 simple vector (TsingKe Biotech, Beijing, China) for TA cloning (TA is short for thymine and adenine). Ligation products were transformed into the *Escherichia coli* strain DH5 α , and single colonies were selected for plasmid isolation and DNA sequencing.

Morphological properties of barley grains

The phenotypic observation of grain development in wild-type barley and mutants (*hvhpt15* and *hvhgg13*) was performed at 1, 2, 3 and 4 weeks after pollination. Whole grains or dehusked grains and their longitudinal section were imaged with a trinocular stereo microscope (Nikon, SMZ745T, Japan). Mature grains from gRNA/Cas9 transgene-free, homozygous T₂ mutant lines were used for the analysis of grain width (with ImageJ software) and thousand-grain weight.

Mature barley grains were fractured transversely using a razor blade and tweezers. The resulting cross-sections of wild-type barley grains (outer endosperm regions) and their mutants were fixed on an aluminium specimen holder with double graphite tape. Samples were sputter-coated (Hitachi E-1010, Japan) with gold and examined with a scanning electron microscope (Hitachi S-3000N) at 20 kV at room temperature of 25 °C.

Measurement of starch content

Total starch content was determined enzymatically using the Total Starch Analysis Kit (Megazyme, Bray, Ireland). The amylose content was assayed with the Amylose/Amylopectin Assay Kit (Megazyme) based on the glucose oxidase–peroxidase method, as recommended by the manufacturer.

Gene expression analysis

Tissues from wild-type and transgenic lines were homogenized in liquid nitrogen, and then total RNA was prepared with an EZNA Plant RNA kit following the manufacturer’s instructions (Omega, Norcross, GA, USA). One microgram of total RNA was digested with a gDNA Remover Kit and reversely transcribed into cDNA in ReverTra Ace qPCR RT Master Mix (Toyobo, Kyoto, Japan) in a 20- μ L reaction volume. Transcript analysis was conducted using semi-quantitative reverse transcriptase PCR (RT-PCR), and *HvACTIN* was used as the control gene for all cDNA samples. The primer sequences for all barley genes determined are listed in [Supplementary Data Table S4](#).

Vitamin E measurement by high-performance liquid chromatography (HPLC)

Vitamin E was extracted according to previously described methods, with minor modifications (Chen *et al.*, 2017). Leaves

or mature grains of barley were ground to a fine powder in liquid nitrogen, and 50 mg of powder was extracted in 1.5 mL methanol by vortexing vigorously for 10 min at room temperature. The samples were centrifuged at 10 000 *g* for 5 min, and the supernatant was transferred to a new tube. The pellet was re-extracted twice. All three supernatants were pooled, filtered through a 0.22- μ m membrane, and dried under a vacuum using a centrifugal evaporator (Labconco). The residues were dissolved in 100 μ L methanol/isopropanol (1 : 1, v/v) and centrifuged at 14 000 *g* for 5 min. Vitamin E was determined using an Agilent 1200 HPLC (Agilent Technologies) equipped with a Phenomenex Kinetex F5 100A column (2.6 μ m, 150 \times 4.6 mm; Phenomenex) and a G1321A fluorescence detector. The mobile phase used was methanol/H₂O (85 : 15, v/v) at a flow rate of 1.0 mL min⁻¹. Sample components were detected by fluorescence with excitation at 298 nm and emission at 328 nm (Greibenstein and Frank, 2012). Tocopherols and tocotrienols were quantified against external standard curves using authentic compounds (ChromaDex).

Phylogenetic analysis

The amino acid sequences of HPTs and HGGTs from eight plant species (*Hordeum vulgare*, *Triticum aestivum*, *Zea mays*, *Oryza sativa*, *Arabidopsis thaliana*, *Sorghum bicolor*, *Brachypodium distachyon* and *Avena sativa*) were used to construct a phylogenetic tree. The accession numbers for these sequences were retrieved from the Phytozome (v12.1.6), UniProtKB or NCBI database. Multiple sequence alignments were performed using the Clustal Omega program (<https://www.ebi.ac.uk/Tools/msa/clustalo/>), and subsequent phylogenetic analysis was conducted using the maximum-likelihood method in the MEGA7 program.

Transient gene expression in tobacco leaves

A full-length coding sequence of an HPT homologue (*HORVU2Hr1G117600*) was amplified (primers are listed in Supporting Data Table S3) using RT-PCR from mRNAs extracted from grains (14 d after pollination) of barley ('Morex') and cloned into the pH7FWG2.0 vector under control of the 35S promoter. The resulting DNA construct was electroporated into *Agrobacterium tumefaciens* strain EHA105. *Agrobacterium* cultures, carrying the empty vector (pH7FWG2.0) and 35S: *HORVU2Hr1G117600* were infiltrated into 1-month-old tobacco (*Nicotiana benthamiana*) leaves using a needleless syringe. The plants were incubated at 24 °C under a 16-h/8-h light–dark cycle. Five days after infiltration, the control and infiltrated leaves were collected for tocochromanol extraction and HPLC analyses.

Statistical analysis

All experiments were repeated at least three times. The data shown represent the mean \pm s.e. Asterisks indicate a

significant difference between the wild-type and mutant plants at **P* < 0.05 or ***P* < 0.01, as determined by Student's *t*-tests.

RESULTS

Design and delivery of PTG editing constructs into barley plants

Genomic sequences of barley HPT (*HvHPT*, *HORVU7Hr1G110990*) and HGGT (*HvHGGT*, *HORVU7Hr1G114330*) genes from the Ensembl Plants database showed that *HvHPT* (6481 bp) has 12 exons and 11 introns and that *HvHGGT* (4747 bp) has 14 exons and 13 introns (Fig. 1A, B). To effectively carry out targeted mutations of these two genes, four single gRNAs were designed to target specific sites in the protein-coding region with low sequence homology (Fig. 1A, B; Supplementary Data Fig. S1A). gRNA1 and gRNA2 were expected to target the first and second exons of *HvHPT*, respectively, whereas gRNA3 and gRNA4 were designed to target the first two exons of *HvHGGT*. As shown in Fig. 1C, two gRNAs were assembled into a single vector using the polycistron tRNA–gRNA (PTG) strategy (Xie *et al.*, 2015), generating two constructs, *PTG-HPT/Cas9* and *PTG-HGGT/Cas9* (Table S2), for barley transformation and genome editing. The two constructs were independently transformed into immature barley embryos via *Agrobacterium*-mediated transformation. We obtained ~700 and 550 embryo-derived calli exhibiting hygromycin resistance for the *PTG-HPT/Cas9* and *PTG-HGGT/Cas9* constructs, respectively. A total of 26 primary plantlets for *PTG-HPT/Cas9* and 17 for *PTG-HGGT/Cas9* were regenerated from the transformed calli (Table S5).

Targeted mutagenesis of *HvHPT* and *HvHGGT* induced by CRISPR/Cas9 in the T₀ generation

To examine targeted mutagenesis in T₀ plants, the targeted protospacer regions of *HvHPT* and *HvHGGT* were amplified by PCR for DNA sequencing (10–15 amplicons per primary mutant plant; see Supplementary Data Table S3 for primer sequences), and the resulting sequences were aligned against the wild-type DNA sequence. The sequencing data revealed 13 mutant lines for *Hvhpt* and 11 for *Hvhggt* (Table S5). Mutagenesis efficiency among T₀ regenerated plantlets was 50–65 % as a result of two simultaneously expressed gRNAs targeting each gene. In the *PTG-HPT/Cas9* transgenic lines (Fig. 2A), site-specific indels (insertions and deletions) occurred at 0–7 bp upstream of the protospacer-adjacent motif (PAM) or at imprecise sites, thus eliminating PAMs or a genomic sequence far from PAMs. A fragment deletion of up to 746 bp at a single target site was also observed in line *hpt15*. Among the 13 *Hvhpt* mutant lines, targeted mutagenesis at gRNA1 target sites was much higher than that at gRNA2 sites (Fig. 2A), indicating wide variation in gRNA1 and gRNA2 mutagenic efficiency. In the *PTG-HGGT/Cas9* primary transgenic lines (Fig. 2B), single-base substitutions or small indels (+1, –1 or –2 bp) were only observed at the gRNA4 target site. Notably, all of these small indels occurred specifically 3 bp upstream of the PAM. Among all T₀ *Hvhggt* mutant plants, no mutation was detected at the gRNA3 target site

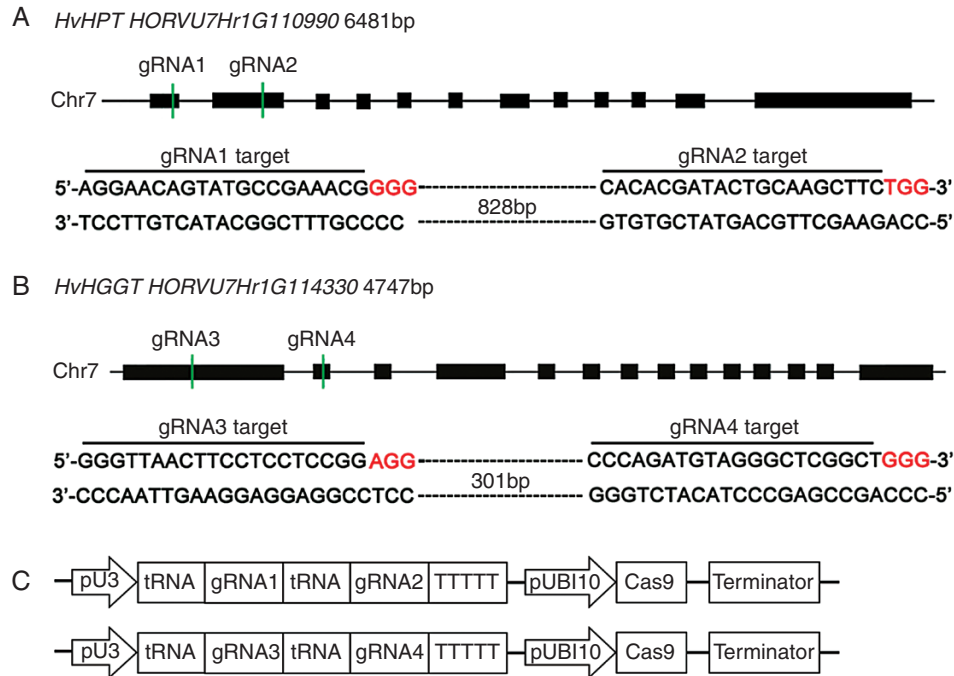


FIG. 1. Schematic diagram of *HvHPT* and *HvHGGT* genes targeted by four specific gRNAs. (A) Gene structure of *HvHPT* with gRNA1 and gRNA2 targeting sites. The distance between the two target sites is 831 bp. (B) Gene structure of *HvHGGT* with gRNA3 and gRNA4 targeting sites. The distance between the two target sites is 304 bp. (C) Schematic of the tRNA–gRNA fragments inserted into the pRGEb32 vector. Black rectangles indicate protein-coding regions. The PAM, protospacer-adjacent motif, is shown in red. The green vertical lines indicate the relative location of gRNA targeting sites; the overlined nucleotides indicate the target sequence for each gRNA. pUBI10, rice ubiquitin promoter; pU3, rice U3 snoRNA promoter.

(Fig. 2). In general, the mutations induced in the barley *HvHPT* and *HvHGGT* genes consisted predominantly of 1-bp indels.

Quantitative analysis of the T_0 mutant plants showed that the mutation rate induced by gRNA4 (64.7 %) was much higher than those induced by gRNA1 (46.2 %) and gRNA2 (11.5 %) and that gRNA3 did not induce indels at the target site (Table 1). No homozygous mutations were identified in T_0 mutant plants (Table 1). As heterozygous plants may also be chimeric, heterozygosity and chimerism cannot readily be distinguished in a given plant. Therefore, all of the primary mutant lines for *Hvhpt* and *Hvhggt* were categorized as heterozygous/chimeric. These results indicated a high percentage of heterozygous/chimeric mutants in the T_0 generation and that the four gRNAs varied in genome-editing performance, suggesting that gRNA design is important for mutagenesis efficiency.

Characterization of chimeric lines in T_0 transgenic plants and selection of ‘transgene-free’ homozygous barley mutants

To investigate whether chimeras were present in a tiller or multiple tillers of a mutant line, genomic DNA from four different tillers of each T_0 mutant plant was extracted, and the target sites were individually sequenced (Fig. 3A). The wild-type sequence was found in all tillers (Fig. 3B, C). In line *hpt11*, mutation types varied among the four tillers, but each tiller had only one mutation type (Fig. 3B). This result suggested the existence of chimeras among the different tillers. However, one to five different mutation types were detected in individual tillers of the line *hggt15* (Fig. 3C), suggesting that this phenomenon

could be present not only in different tillers but also in leaves from the same tiller. Among 13 *hpt* mutants and 11 *hggt* mutants, at least seven lines were chimeric (Fig. 2). Overall, more than half of the mutant plants were chimeric, and chimeras were found in the same tiller or different tillers.

Because chimeras were observed in T_0 transgenic lines, the inheritance and consistency of targeted mutations were further analysed in the T_1 generation. To assess whether the gRNA/Cas9 transgene was able to induce new mutations in progeny plants, we chose seedlings of the T_1 generation that were derived from one tiller of a chimeric primary transgenic line (*hggt15-3*) (Fig. 3C). Most mutation types of the T_0 plants were faithfully inherited in the T_1 generation, such as a 1-bp (+A, +T or +C) insertion (Supplementary Data Fig. S2). However, not all mutation types were transmitted from the T_0 to T_1 generation, including base substitutions (A/G and G/A), which were not detected in the latter generation (Fig. S2). Notably, trans-generational editing occurred in T_1 plants, and the presence of the gRNA/Cas9 transgene induced new mutation types at target sites, including 1- to 5-bp deletions (–G, –CG, –GCCG, –GGCTC), 2-bp insertions (+TT) and T/C substitutions, although no new mutations occurred in transgene-free plants (Fig. S2). Therefore, plants with the gRNA/Cas9 transgene displayed more mutation types compared with the gRNA/Cas9-free plants, suggesting that it is necessary to obtain transgene-free plants for fixed mutations.

To avoid possible new mutation types produced in gRNA/Cas9 transgenic plants, homozygous mutations for *HvHPT* or *HvHGGT* without any transgenic elements were screened in the T_1 plants via PCR and DNA sequencing. Among at least 44

A *Hvhpt-T0*

	gRNA1 target	gRNA2 target	gRNA1	gRNA2
WT	5'-CTTTCCGGAATAGGAACAGTATGCCGAAACGCGG-----CACACGATACTGCAAGCTTCGGAAGCCAA-3'			
<i>hpt2</i>	CTTTCCGGAATAGGAACAGTATGCCGAA ^{laggaacacca} CG _g GGG-----CACACGATACTGCAAACTTCGGAAGCCAA		A/G, +12bp	G/A
	CTTTCCGGAATAGGAACAGTATGCCGAA_CG _g GGG-----CACGATACTGCAAGCTTCGGAAGCCAA		-1bp	A/G
	CTTTCCGGAATAGGAACAGTATGCCGAAACGCGG-----CACAC-----CAA		0	delete 22bp
<i>hpt3</i>	CTTTCCGGAATAGGAACAGTATGCCGAA ^{laggaacacca} CG _g GGG-----CACACGATACTGCAAGCTTCGGAAGCCAA		A/G,+12bp	0
<i>hpt5</i>	CTTTCCGGAATAGGAACAGTATGCCG_AACG _g GGG-----CACACGATACTGCAAGCTTCGGAAGCCAA		-1bp	0
	CTTTCCGGAATAGGAACAGTATGCCG _a AACG _g GGG-----CACACGATACTGCAAGCTTCGGAAGCCAA		+1bp	0
<i>hpt7</i>	CTTTCCGGAATAGGAACAGTATGCCG_AACG _g GGG-----CACACGATACTGCAAGCTTCGGAAGCCAA		-1bp	0
<i>hpt8</i>	CTTTCCGGAATAGGAACAGTATGCCG_AACG _g GGG-----CACACGATACTGCAAGCTTCGGAAGCCAA		-1bp	0
<i>hpt10</i>	CTTTCCGGAATAGGAACAGTATGCCG _a AACG _g GGG-----CACACGATACTGCAAGCTTCGGAAGCCAA		+1bp	0
	CTTTCCGGAATAGGAACAGTATGCCG _a AACG _g GGG-----CACACGATACTGCAAGCTTCGGAAGCCAA		-1bp	0
<i>hpt11</i>	CTTTCCGGAATAGGAACAGTATGCCG _a AACG _g GGG-----CACACGATACTGCAAGCTTCGGAAGCCAA		+1bp	0
	CTTTCCGGAATAGGAACAGTATGCCG_AACG _g GGG-----CACACGATACTGCAAGCTTCGGAAGCCAA		-1bp	0
	CTTTCCGGAATAGGAACAGTATGCCG _a AACG _g GGG-----CACACGATACTGCAAGCTTCGGAAGCCAA		A/G	0
<i>hpt13</i>	CTTTCCGGAATAGGAACAGTATGCCG_AACG _g GGG-----CACACGATACTGCAAGCTTCGGAAGCCAA		-1bp	0
	CTTTCCGGAATAGGAACAGTATGCCG ^{laggaacacca} CG _g GGG-----CACACGATACTGCAAGCTTCGGAAGCCAA		A/G,+12bp	0
<i>hpt14</i>	CTTTCCGGAATAGGAACAGTATGC-----G-----CACACGATACTGCAAGCTTCGGAAGCCAA		-9bp	0
<i>hpt15</i>	CT-----ACCGTT-----CACACGATACTGCAAG-----GAAGCCAA		delete 746bp	-6bp
<i>hpt18</i>	CTTTCCGGAATAGGAACAGTATGCCGAAACGCGG-----CACACGATACTGCAAA_TTTCGGAAGCCAA		0	-2bp
<i>hpt20</i>	CTTTCCGGAATAGGAACAGTATGC-----G-----CACACGATACTGCAAGCTTCGGAAGCCAA		-9bp	0
	CTTTCCGGAATAGGAACAGTATCGC-----G-----CACACGATACTGCAAGCTTCGGAAGCCAA		T/C,-9bp	0
<i>hpt23</i>	CTTTCCGGAATAGGAACAGTATGCCG_AACG _g GGG-----CACACGATACTGCAAGCTTCGGAAGCCAA		-1bp	0
	CTTTCCGGAATAGGAACAGTATGC-----G-----CACACGATACTGCAAGCTTCGGAAGCCAA		-9bp	0
	CTTTCCGGAATAGGAACAGTATCCGAAACGCGG-----CACACGATACTGCAAGCTTCGGAAGCCAA		G/A	0

B *Hvhggt-T0*

	gRNA3 target	gRNA4 target	gRNA3	gRNA4
WT	5'-CGCGGGTAACTTCTCTCTCCGGAGG-----AGGGCCAGATGTAGGGCTCGGCTGGGAACGAC-3'			
<i>hgt3</i>	CGCGGGTAACTTCTCTCTCCGGAGG-----AGAGGGCCAGATGTAGGGCTCG _g GCTGGGAACGAC		0	+1bp
<i>hgt5</i>	CGCGGGTAACTTCTCTCTCCGGAGG-----AGAGGGCCAGATGTAGGGCTCG _g GCTGGGAACGAC		0	+1bp
	CGCGGGTAACTTCTCTCTCCGGAGG-----AGAGGGCCAGATGTAGGGCTCG _a GCTGGGAACGAC		0	+1bp
	CGCGGGTAACTTCTCTCTCCGGAGG-----AGAGGGCCAGATGTAGGGCTC_GCTGGGAACGAC		0	-1bp
	CGCGGGTAACTTCTCTCTCCGGAGG-----AGAGGGCCAGATGTAGGGCT__GCTGGGAACGAC		0	-2bp
	CGCGGGTAACTTCTCTCTCCGGAGG-----AGAGGGCCAGATGTAGGGCTCG _g GCTGGGAACGAC		0	A/G
<i>hgt6</i>	CGCGGGTAACTTCTCTCTCCGGAGG-----AGAGGGCCAGATGTAGGGCTCG _g GCTGGGAACGAC		0	+1bp
	CGCGGGTAACTTCTCTCTCCGGAGG-----AGAGGGCCAGATGTAGGGCTC_GCTGGGAACGAC		0	-1bp
	CGCGGGTAACTTCTCTCTCCGGAGG-----AGAGGGCCG _g GATGTAGGGCTCG _g GCTGGGAACGAC		0	A/G,+1bp
	CGCGGGTAACTTCTCTCTCCGGAGG-----AGAGGGCCAGATGTAG _g GCTC_GCTGGGAACGAC		0	G/T,-1bp
<i>hgt8</i>	CGCGGGTAACTTCTCTCTCCGGAGG-----AGAGGGCCAGATGTAGGGCTCG _a GCTGGGAACGAC		0	+1bp
<i>hgt9</i>	CGCGGGTAACTTCTCTCTCCGGAGG-----AGAGGGCCATAGATGTAGGGCTCGGCTGGGAACGAC		0	C/T
<i>hgt10</i>	CGCGGGTAACTTCTCTCTCCGGAGG-----AGAGGGCCAGATGTAGGGCTCG _g GCTGGGAACGAC		0	+1bp
	CGCGGGTAACTTCTCTCTCCGGAGG-----AGAGGGCCAGATGTAGGGCTCG _g GCTGGGAACGAC		0	+1bp
	CGCGGGTAACTTCTCTCTCCGGAGG-----AGAGGGCCAGATGTAGGGCTC_GCTGGGAACGAC		0	-1bp
	CGCGGGTAACTTCTCTCTCCGGAGG-----AGAGGGCCAGATGTAGGGCTCG _g GCTGGGAACGAC		0	+1bp
	CGCGGGTAACTTCTCTCTCCGGAGG-----AGAGGGCCAGATGTAGGGCTCG _g GCTGGGAACGAC		0	+1bp
	CGCGGGTAACTTCTCTCTCCGGAGG-----AGAGGGCCAAATGTAGGGCTC_GCTGGGAACGAC		0	G/A,-1bp
<i>hgt12</i>	CGCGGGTAACTTCTCTCTCCGGAGG-----AGAGGGCCAGATGTAGGGCCCGGCTGGGAACGAC		0	T/C
	CGCGGGTAACTTCTCTCTCCGGAGG-----AGAGGGCCAGATGTAGGGCTCG _g GCTGGGAACGAC		0	+1bp
	CGCGGGTAACTTCTCTCTCCGGAGG-----AGAGGGCCAGATGTAGGGCT__GCTGGGAACGAC		0	-2bp
	CGCGGGTAACTTCTCTCTCCGGAGG-----AGAGGGCCAGATGTAGGGCTC_GCTGGGAACGAC		0	-1bp
<i>hgt13</i>	CGCGGGTAACTTCTCTCTCCGGAGG-----AGAGGGCCAGATGTAGGGCTCG _g GCTGGGAACGAC		0	+1bp
<i>hgt14</i>	CGCGGGTAACTTCTCTCTCCGGAGG-----AGAGGGCCAGATGTAGGGCTCG _g GCTGGGAACGAC		0	+1bp
	CGCGGGTAACTTCTCTCTCCGGAGG-----AGAGGGCCG _g GATGTAGGGCTC_GCTGGGAACGAC		0	A/G,-1bp
	CGCGGGTAACTTCTCTCTCCGGAGG-----AGAGGGCCAGATGTAGGGCTCG _g GCTGGGAACGAC		0	+1bp
	CGCGGGTAACTTCTCTCTCCGGAGG-----AGAGGGCCAGATGTAGGGCTC_GCTGGGAACGAC		0	-1bp
	CGCGGGTAACTTCTCTCTCCGGAGG-----AGAGGGCCAGATGTAGGGCTCG _g GCTGGGAACGAC		0	+1bp
<i>hgt15</i>	CGCGGGTAACTTCTCTCTCCGGAGG-----AGAGGGCCAGATGTAGGGCTCG _g GCTGGGAACGAC		0	+1bp
	CGCGGGTAACTTCTCTCTCCGGAGG-----AGAGGGCCAGATGTAGGGCTCG _g GCTGGGAACGAC		0	C/G,+1bp
	CGCGGGTAACTTCTCTCTCCGGAGG-----AGAGGGCCG _g GATGTAGGGCTCGGCTGGGAACGAC		0	A/G
	CGCGGGTAACTTCTCTCTCCGGAGG-----AGAGGGCCAGATGTAGGGCTC_GCTGGGAACGAC		0	-1bp
	CGCGGGTAACTTCTCTCTCCGGAGG-----AGAGGGCCAGATGTAGGGCTCG _g GCTGGGAACGAC		0	+1bp
	CGCGGGTAACTTCTCTCTCCGGAGG-----AGAGGGCCG _g GATGTAGGGCTCG _g GCTGGGAACGAC		0	A/G,+1bp
	CGCGGGTAACTTCTCTCTCCGGAGG-----AGAGGGCCAGATGTAGGCTCGGCTGGGAACGAC		0	G/A
	CGCGGGTAACTTCTCTCTCCGGAGG-----AGAGGGCCAGATGTAGGGCTCG _g GCTGGGAACGAC		0	+1bp

Fig. 2. Mutation types in primary transgenic plants revealed by DNA sequencing. (A) Mutant genotypes at gRNA1 and gRNA2 target sites (targeting *HvhPT*). (B) Mutant genotypes at gRNA3 and gRNA4 target sites (targeting *HvhGgt*). WT, wild-type; target sites are shown in green type; single-base substitutions are shown in blue type; the PAM motif is shown in red type; insertions are shown with lowercase letters (subscript); and deletions are indicated by underscoring.

TABLE 1. The mutagenesis frequencies of *HvHPT* and *HvHGGT* gene mutations in the T_0 generation.

Gene	gRNA ID	WT	Homozygous	Heterozygous/ chimeric
<i>HvHPT</i>	gRNA1	53.8 %	ND	12 (46.2 %)
	gRNA2	88.5 %	ND	3 (11.5 %)
<i>HvHGGT</i>	gRNA3	0	ND	ND
	gRNA4	35.3 %	ND	11 (64.7 %)

ND, not detected.

plants of each T_1 line tested, 12–27 plants without the Cas9 transgene were obtained for each mutant line (Table 2). There were 14 Cas9-free homozygotes for *hpt* mutants, including seven *hpt15* plants [large-fragment deletion (–746 bp)], five *hpt14* plants [9-bp deletion (–CGAAACGGG)] and two *hpt11* plants [1-bp indel (+G or –A)]. The number of Cas9-free homozygotes for *hgg15*, *hgg10*, *hgg13* and *hgg15* lines were 15, 14, 15 and seven, respectively (Table 2). Notably, all of the transgene-free *hgg15* homozygotes displayed only a 1-bp indel (+T, +A, or –G). Therefore, ‘transgene-free’ homozygous *Hvhpt* and *Hvhgg15* mutants with different mutation types were obtained in the T_1 generation.

Amino acid sequence analysis and phenotypic observation of *Hvhpt* and *Hvhgg15* homozygous mutants

DNA sequencing analysis showed that *hpt11* carried a single nucleotide insertion, leading to a nonsense mutation at amino acid (aa) 14 (GAA to TGA; Glu to stop) of the 399-residue polypeptide (Fig. 4A). For *hpt15*, a 50-aa deletion occurred at amino acid position 3 and a 2-aa deletion occurred at amino acid 94 (Fig. 4A). Regarding *hgg13* and *hgg15*, a single nucleotide insertion of A or T resulted in a nonsense mutation at amino acid 56 (AAA to TAA, Lys to stop) of the 408-residue polypeptide (Fig. 4A). These deletion, frameshift or in-frame mutations caused truncation near the N-terminus or led to missense mutations in the respective peptides. These two transgene-free homozygous *hpt* lines (*hpt11* and *hpt15*) and two *hgg15* mutant lines (*hgg13* and *hgg15*) were used for further study.

Phenotypic observation of T_1 mutant plants revealed that the developing grains of the *hgg13* homozygous mutant possessed a severely shrunken phenotype, whereas the grain size of the *hpt15* mutant was slightly reduced in comparison to that of the wild-type (Fig. 4B). Further analysis of the mature grains showed that the average grain width decreased by 3–4 % in *hpt* mutants and by 15–19 % in *hgg15* mutants compared to that of the wild-type (Fig. 4C). Moreover, 1000-grain weights were decreased by 5–11 % in *hpt* mutants and by 37–38 % in *hgg15* mutants (Fig. 4D). Therefore, both homozygous mutations, particularly the *Hvhgg15* mutation, significantly decreased grain size and weight, indicating a significant role of *HvHPT* and *HvHGGT* in barley grain development.

Additionally, scanning electron microscopy of cross-sections of the grains showed that the grain husk of *hgg15* mutants was shrunken in comparison with that of the wild-type and *hpt* (Fig. 5A, C, E). Furthermore, the starch granules of *hgg15* mutants were irregularly arranged compared with

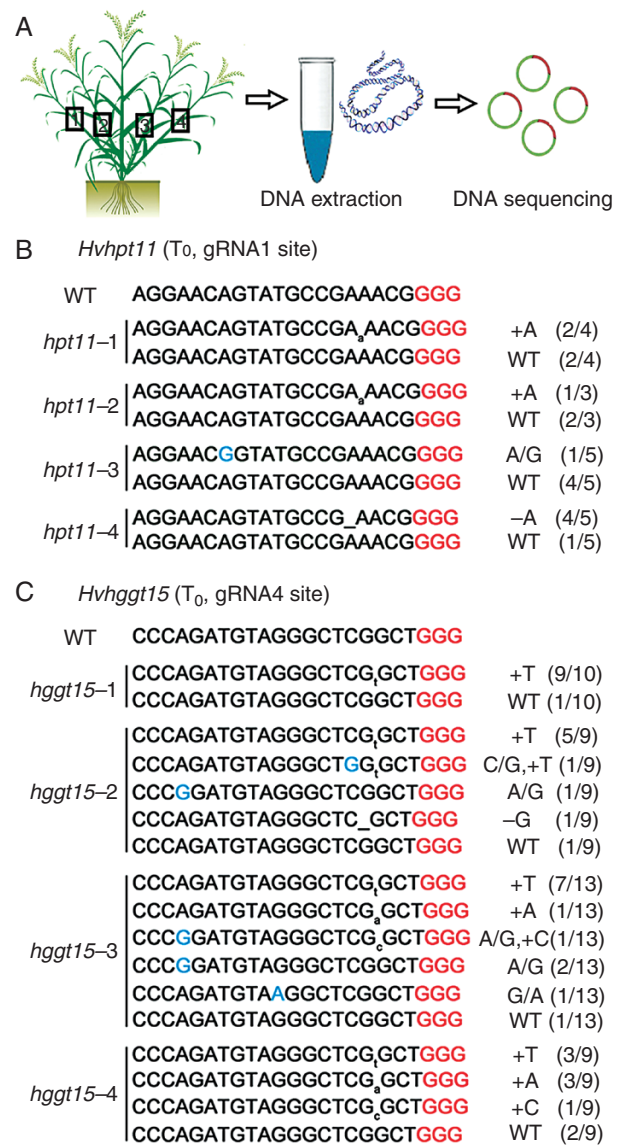


FIG. 3. Primary transgenic plants are mostly chimeric at the target sites of *HvHPT* or *HvHGGT*. (A) Extraction of genomic DNA from four different tillers of each mutant plant for sequencing. (B) Mutation patterns of four individual tillers detected in the T_0 *hpt11* mutant. (C) Mutation patterns of four individual tillers detected in the T_0 *hgg15* mutant. WT, wild-type; single-base substitutions are shown in blue type; the PAM motif is shown in red type; insertions are shown with lowercase letters (subscript); and deletions are indicated by underscoring.

that of the wild-type and *hpt* (Fig. 5B, D, F). Because grains consist mainly of starch, we presumed that the shrunken kernel phenotype of the *Hvhgg15* mutant might be related to starch accumulation in barley. To investigate the effects of *HvHPT* and *HvHGGT* mutation on starch levels, the contents of total starch and amylose were determined for the mature barley grains. The results showed that the total starch content decreased significantly by 10–13 % in *hpt* mutants and by 27–30 % in *hgg15* mutants compared with that of the wild-type (Fig. 5G). However, the ratio of amylose to total starch content was not significantly different between that of the wild-type and the mutants (Fig. 5H). The above results

TABLE 2. Selection and characterization of 'transgene-free' homozygous barley mutants

T-DNA constructs	T ₁ mutant lines	No. of plants tested	No. of Cas9-free plants	No. of heterozygotes (Cas9-)	No. of homozygotes (Cas9-)	Mutation pattern of homozygotes (Cas9-)
PTG-HPT/Cas9	<i>hpt11</i>	146	27	4	2	+1 bp (+G); -1 bp (-A)
	<i>hpt14</i>	54	12	7	5	-9 bp (-CGAAACGGG)
	<i>hpt15</i>	48	21	13	7	-746 bp (large-fragment deletion)
PTG-HGGT/Cas9	<i>hgg15</i>	52	15	0	15	+1 bp (+A); +1 bp (+T); -1 bp (-G)
	<i>hgg10</i>	50	16	2	14	+1 bp (+A); -1 bp (-G); +1 bp (+A)/ -1 bp (-G)
	<i>hgg13</i>	44	15	0	15	+1 bp (+T)
	<i>hgg15</i>	54	17	4	7	+1 bp (+A)

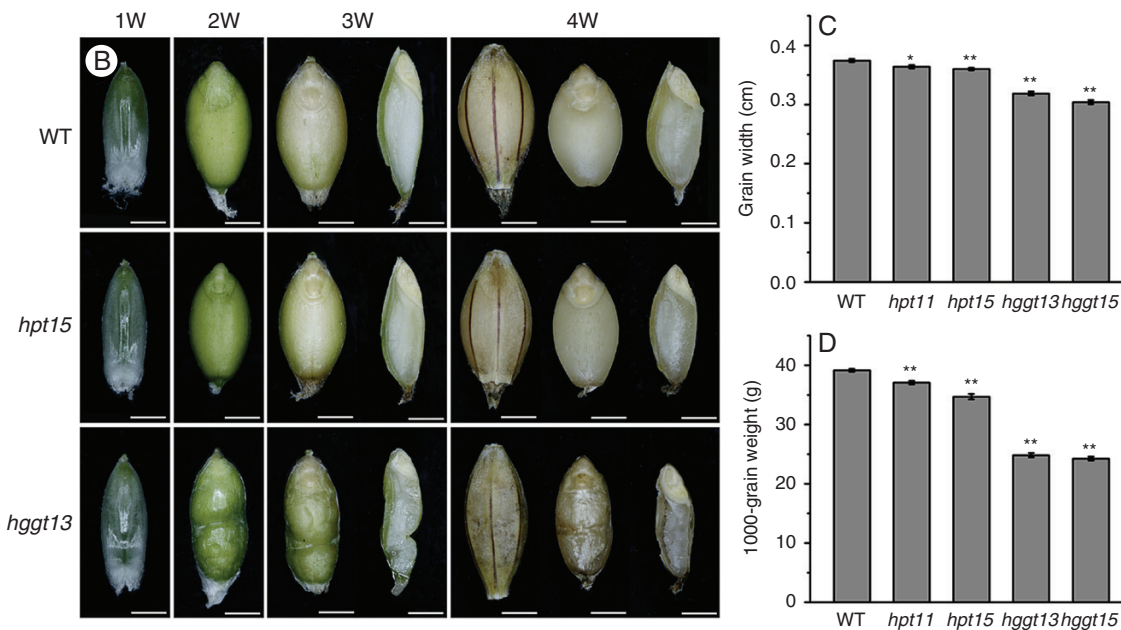
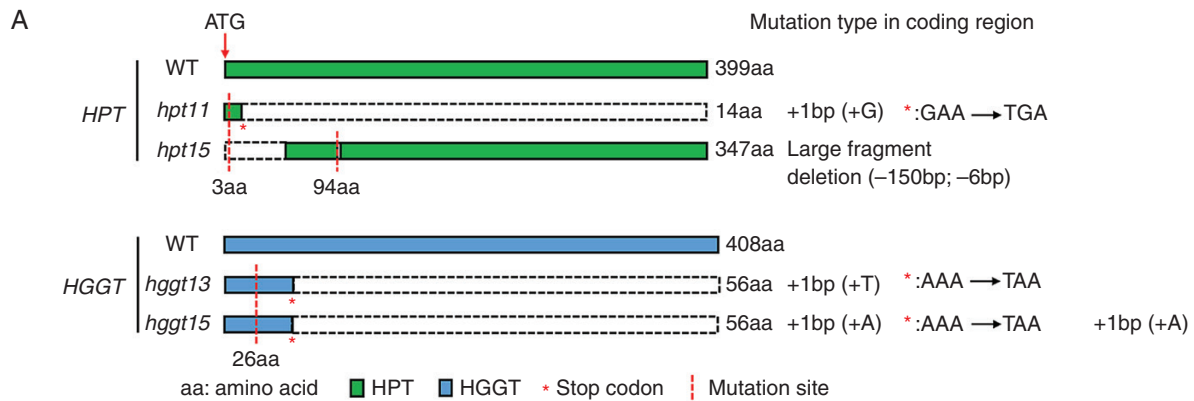


FIG. 4. Amino acid sequence analysis and grain phenotypic observation of barley *hpt* and *hgg1* mutants. (A) Amino acid sequence analysis of barley *hpt* and *hgg1* mutants. (B) Developing grains of the wild-type (WT) and mutants (*hvhpt15* and *hvhgg13*). (C) Grain width (cm). (D) Thousand-grain weight (g). Phenotypic observation of grain development was performed at 1, 2, 3 and 4 weeks (W) after pollination. Whole grains or dehusked grains and their longitudinal section were imaged with a trinocular stereo microscope. Mature grains of transgene-free, homozygous T₂ mutant lines were used for the analysis of grain width (with ImageJ software) and thousand-grain weight. Means and s.e. of at least three replicates are presented, with $n > 45$ for each repeat. Asterisks indicate a significant difference between the wild-type and mutant lines at * $P < 0.05$ or ** $P < 0.01$, as determined by Student's *t*-tests. Scale bars = 2.6 mm.

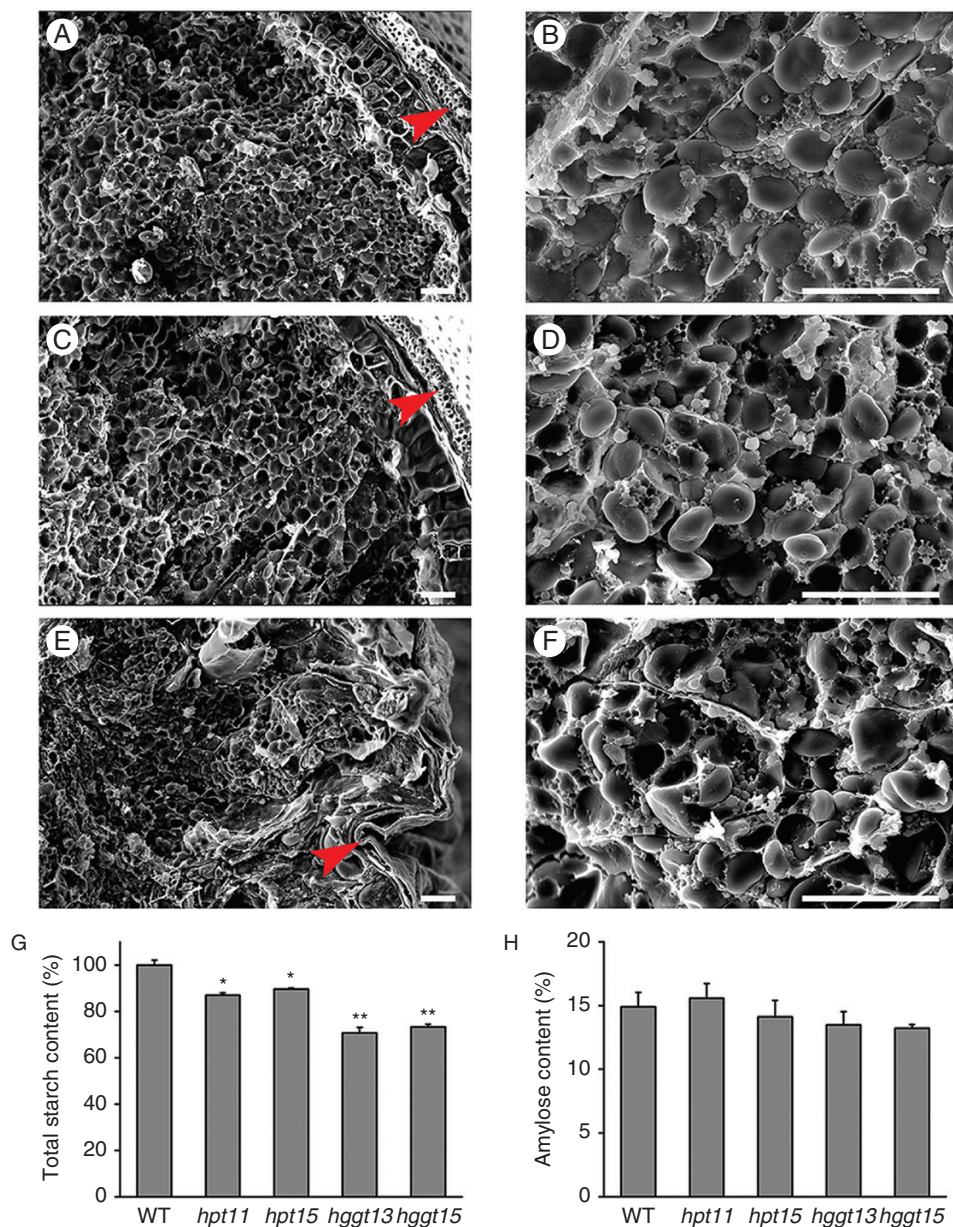


FIG. 5. Morphology of cross-section of grains and the content of total starch and amylose in barley. Scanning electron micrographs of barley grains in the wild-type (WT) (A and B), *hpt* (C and D), and *hggT* (E and F) mutants. (G) Total starch content (%). (H) Amylose content (%). Mature grains of the WT, and *hpt* and *hggT* mutants were used for microscopy and starch content measurement. Means and s.e. of at least three replicates are presented. Asterisks indicate a significant difference between the WT and mutants at **P* < 0.05 or ***P* < 0.01, as determined by Student's *t*-tests. Red arrowheads, grain husk. Scale bars = 50 μm.

suggested that *HvHGGT* is involved in starch accumulation in barley grains.

CRISPR/Cas9-induced mutations significantly altered vitamin E contents in mature grains of *T₂* homozygous mutants

To investigate whether CRISPR/Cas9-mediated targeted mutagenesis of *HvHPT* and *HvHGGT* affected the vitamin E metabolic pathway, tocopherols were extracted from the *T₂* mature grains of homozygous mutants and analysed using HPLC for the contents of eight vitamin E isomers (Fig. 6A-E).

As shown in Fig. 6A, the peaks of the eight isomers varied greatly in wild-type barley (the peaks for γ and α isomers were predominant, whereas the δ and β peaks were much smaller). Peaks in the *hpt11* and *hpt15* mutant lines were similar (Fig. 6B, C). The peaks for γ -T and α -T were smaller than those in the wild-type, and a modest decline was observed for δ -T3, β -T3, γ -T3 and α -T3 peaks. Notably, peaks for the four isomers of tocotrienol were almost undetectable in both the *hggT13* and the *hggT15* mutant lines, whereas peaks for the four isomers of tocopherol were similar to those in the wild-type (Fig. 6A, D, E).

Quantitative analysis confirmed that α -T3 was the predominant form of vitamin E in wild-type barley, followed by γ -T3, α -T, γ -T

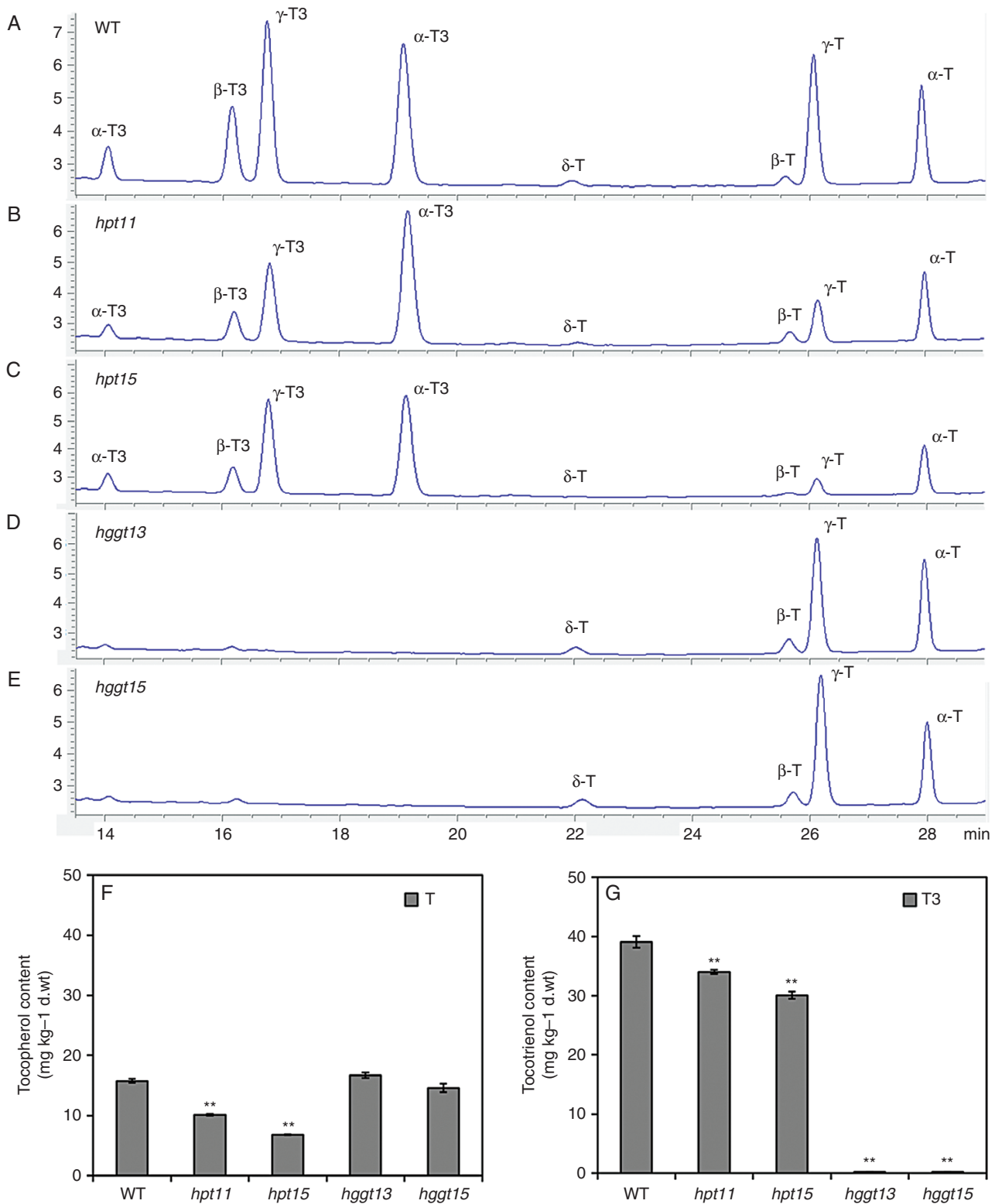


FIG. 6. Tocopherol and tocotrienol levels in mature grains of *Hvhpt* and *Hvhggt* T_2 mutant lines. (A–E) HPLC profiles of tocopherol and tocotrienol isomers in the wild-type, and *hpt* and *hgg1* mutants. (F) The content of tocopherol (T). (G) The content of tocotrienol (T3). Mature grains of transgene-free homozygous T_2 mutant lines were used for measurements and 50 mg of grain powder was used in each replicate. Means and s.e. of at least three replicates are presented. Asterisks indicate a significant difference between the wild-type and mutant lines at * $P < 0.05$ or ** $P < 0.01$, as determined by Student's *t*-tests.

and β -T3 and that the contents of the β -T and δ isoforms were very low (Supplementary Data Table S6). Mutations in *HvHPT* significantly decreased the tocopherol content by 36–57 % and tocotrienol content by 13–23 % (Fig. 6F, G). Isoforms α and γ were still the major isoforms of vitamin E in lines *hpt11* and *hpt15*, and the contents of α -T, γ -T and γ -T3 were reduced by 25–43, 68–88 and 32–50 %, respectively (Table S6). In contrast, no significant difference was observed for α -T and γ -T contents in *HvHGGT* mutant lines compared with that of the wild-type (Fig. 6F; Table S6). Because α -T and γ -T account for 95 % of the total tocopherols, we found no significant difference in total tocopherol content between wild-type and *hggT* mutants. Nonetheless, the tocotrienol content did decrease to almost zero in the *hggT* mutant lines (Fig. 6G), indicating that *HvHGGT* is the gene responsible for the synthesis of tocotrienols in barley grains. Indeed, the mutation in *HvHGGT* almost completely blocked tocotrienol biosynthesis but did not affect tocopherol biosynthesis. In contrast, the mutation in *HvHPT* did not completely block tocopherol biosynthesis in barley grains. One possible explanation is the existence of an *HPT* homologue or the existence of other pathway genes in the barley genome that contribute to tocopherol biosynthesis.

Phylogenetic and functional analyses of HPT and HGGT homologue genes in barley

To determine whether an unknown homologue of *HvHPT* for tocopherol biosynthesis exists in the barley genome, we searched the barley genome database and identified a coding sequence (*HORVU2Hr1G117600*) that shared 79.8 % nucleotide identity (73.3 % amino acid identity) with *HvHPT* (Supplementary Data Fig. S1B). Furthermore, the translated amino acid sequence contained a UbiA prenyltransferase domain that is conserved in both HPT and HGGT proteins (Fig. S1). Phylogenetic analysis of the amino acid sequences indicated that HPT and HGGT belonged to two specific subgroups with distinct clustering (Fig. S3). Among the eight species examined, HPTs were found in both monocots and dicots, whereas HGGTs were present only in the monocots assessed. The sequence similarity of barley HPT to that of wheat and oat HPT was higher than that of the *Brachypodium*, *Sorghum*, maize and rice genes, although the deduced amino acid sequence of *HORVU2Hr1G117600* was closest to that of the rice HPT among monocots. We isolated the full-length cDNA of *HORVU2Hr1G117600* via reverse transcription from mRNAs extracted from the barley grains (14 d after pollination). To test whether the possible HPT homologue (*HORVU2Hr1G117600*) has a potential role in tocopherol biosynthesis, we performed transient overexpression of *HORVU2Hr1G117600* in tobacco leaves by agro-infiltration. HPLC analysis showed that α -T and γ -T were the major tocopherol isoforms of vitamin E in tobacco leaves, and overexpression of *HORVU2Hr1G117600* significantly increased the production of γ - and δ -tocopherol isoforms (Fig. S4). This result suggested that the HPT homologue (*HORVU2Hr1G117600*) may function in tocopherol biosynthesis in barley grains.

To further determine whether *HORVU2Hr1G117600* or *HGGT* contributes to tocopherol biosynthesis in barley, we examined their expression in the leaves and grains

of *hpt* mutants. The results showed that the expression of *HORVU2Hr1G117600* and *HGGT* was only found in grains, but not in leaves of the wild-type and mutant lines (Supplementary Data Fig. S5A). Furthermore, analysis of leaf tocochromanols showed a significant decrease in the total tocopherol content in line *hpt15* of 41 % of that in the wild-type, and no tocotrienols were detected in *hpt15* or the wild-type (Fig. S5B). Regardless, tocopherols still accumulated in *hvhpt* mutants when *HvHGGT* and *HORVU2Hr1G117600* were not expressed in leaves, suggesting that they may not contribute to vitamin E biosynthesis in barley leaves. Taken this evidence together, *HORVU2Hr1G117600* may share *HvHPT* function in barley grains, but not in leaves, implying that other biosynthesis pathway-related genes might be involved in the accumulation of tocopherols in barley (Fig. 7).

DISCUSSION

Targeted mutagenesis of HPT and HGGT genes in barley via CRISPR/Cas9-mediated genome editing

Barley is a transformation-recalcitrant species, for which genome editing is often an inefficient, laborious and time-consuming process. To improve editing efficiency, we used the PTG strategy (Xie *et al.*, 2015) and employed two gRNAs to target *HvHPT* or *HvHGGT* to increase the success rate. Mutagenesis efficiency among T₀ regenerated plantlets was 50–65 % (Supplementary Data Table S5), which is comparable to that of a previous study on barley using the *Agrobacterium*-mediated transfer of the Cas9 construct, with a frequency of at least 78 % of Cas9-induced mutations in the primary generation (Kapusi *et al.*, 2017), but it is higher than the other three studies in barley, which yielded mutation rates of only 10–23, 44 and 14–25 %, respectively (Lawrenson *et al.*, 2015; Holme *et al.*, 2017; Yang *et al.*, 2020). Another important utility of two gRNAs for targeting one gene is to achieve chromosomal-fragment deletion between two gRNA target sites, which has been shown in barley (Kapusi *et al.*, 2017). In our study, the targeted mutation efficiency of the four gRNAs we designed varied greatly (Table 1). For *HPT*, because the mutation efficiency of gRNA2 was much lower than that of gRNA1, more transgenic lines were needed to increase the odds of achieving fragment deletion. For *HGGT*, gRNA3 caused no indels at the target site. Recently, a transient assay system using protoplasts was used to identify the most effective gRNA candidate or gRNA combinations before transformation (Liang *et al.*, 2017), which would further contribute to improving editing efficiency for crop species, such as maize, barley and wheat.

Stable inheritance of target gene mutations is a major advantage of utilizing the CRISPR/Cas9 system for genome editing and precision breeding. In agreement with the previous studies, we noticed that small indels were the most frequent type of mutation induced by CRISPR/Cas9, and most of the mutations found in T₀ barley plants were inherited by the T₁ generation (Fig. 2; Supplementary Data Fig. S2) (Feng *et al.*, 2014; Zhang *et al.*, 2014; Lawrenson *et al.*, 2015). However, a few mutation types, such as the base substitution (A/G) that occurred in the T₀ generation, were absent in the T₁ generation (Fig. S2). It is possible that this type of mutation existed in somatic cells,

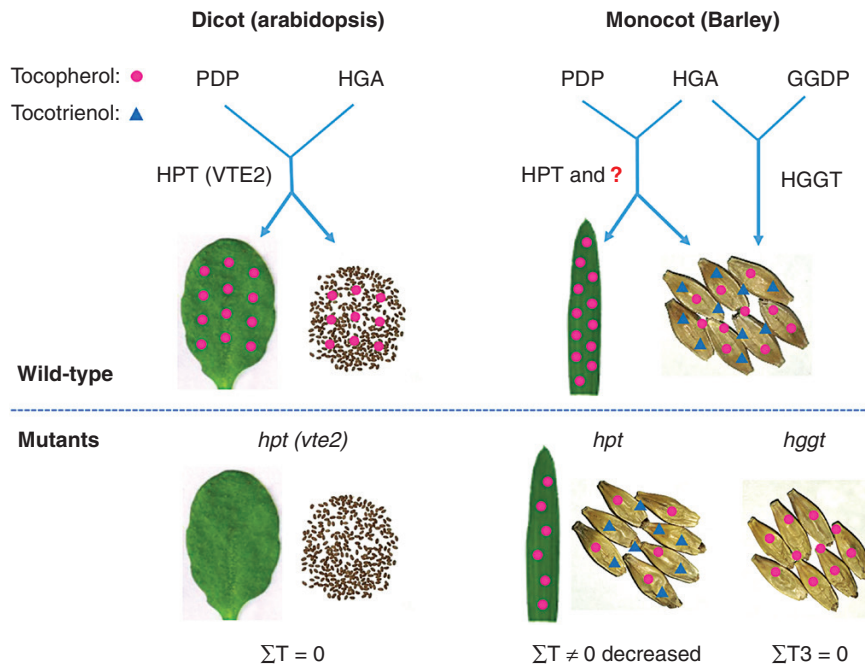


FIG. 7. Vitamin E biosynthesis in barley and *Arabidopsis*. HPT (homogentisate phytyltransferase) and HGGT (homogentisate geranylgeranyl transferase) are the committed-step enzymes for the biosynthesis of tocopherols and tocotrienols, respectively. The question mark indicates an *HPT* homologue or other vitamin E biosynthesis pathway-related genes that may participate in tocopherol production in barley and other monocots. HGA, homogentisate; PDP, phytyl diphosphate; GGDP, geranylgeranyl diphosphate; T, tocopherol; T3, tocotrienol; *hpt*, *HPT* mutant; *vte2*, *HPT* mutant in *Arabidopsis*; *hggT*, *HGGT* mutant. Red circles represent tocopherols; blue triangles represent tocotrienols.

which do not contribute to germ-line development. Because more than half of the T_0 mutant plants were chimeric (Figs 2, 3), the T_1 segregation patterns derived from the T_0 chimeras will be diverse and unpredictable. In the T_0 generation, the CRISPR/Cas9-induced targeted gene modification events may occur relatively late in callus development and/or present multiple cells with different genetic transformation events incorporated during the production of a single transformant. In contrast, transgenic plants with only one type of mutation probably resulting from a single genetic transformation and mutation event occurred in a single embryogenic barley cell.

Additionally, plants with an active gRNA/Cas9 transgene might generate more mutation types than transgene-free plants in subsequent generations (Supplementary Data Fig. S2). Such a situation confirms that the CRISPR/Cas9 system has the sustaining ability to continue gene editing as long as the target site is the wild-type (Feng et al., 2014; Zhang et al., 2014). Usually, gRNA/Cas9 DNA is randomly integrated into the plant genome after entering the nucleus, which may increase the chance of off-target mutation (Lawrenson et al., 2015), induce gene inactivation or instability, and trigger regulatory concerns regarding genetically modified organisms (Jones, 2015). Therefore, it is necessary to remove the gRNA/Cas9 transgene to fix the targeted mutation and to generate transgene-free plants for breeding purposes. Fortunately, exogenous elements, such as single gRNA, Cas9 and the associated selectable marker can be readily removed in later generations via genetic segregation through selfing or backcrossing. Thus far, the CRISPR/Cas9 system has been applied to a variety of plant species to generate transgene-free plants, such as rice (Li et al., 2016; Shen et al., 2018), wheat (Liang et al., 2017) and barley

(Lawrenson et al., 2015; Holme et al., 2017; Kapusi et al., 2017; Yang et al., 2020) among others. In the present study, we successfully performed targeted mutagenesis of two committed genes in vitamin E biosynthesis in barley via CRISPR/Cas9-mediated genome editing. Transgene-free homozygous *Hvhpt* and *HvhggT* mutants could be utilized to understand the genetic control of vitamin E composition in monocots.

Distinctive functions of *HvHPT* and *HvHGGT* in barley vitamin E biosynthesis

In the vitamin E biosynthetic pathway, HPT catalyses the committed step of tocopherol biosynthesis to produce MPBQ, and HGGT catalyses tocotrienol biosynthesis to produce MGGBQ (Schneider, 2005; Chen et al., 2006). Tocopherol biosynthesis has been characterized in the dicot *Arabidopsis thaliana*. Because of the absence of a tocotrienol pathway in *Arabidopsis*, mutations in *HPT* (*VTE2*) result in total tocopherol deficiency in all tissues, as well as reduced seed longevity (Sattler et al., 2004; Yang et al., 2011). In contrast, studies regarding the vitamin E biosynthetic pathway in monocots are extremely limited because of the lack of functional mutants. Our results showed that the *HvHGGT* knockout resulted in undetectable levels of tocotrienols in barley grains without affecting the tocopherol content (Fig. 6), indicating that *HvHGGT* encodes the only committed enzyme that controls the step for GGDP condensation with HGA to produce tocotrienols in barley. Furthermore, the developing grains of *hggT* mutants exhibited a shrunken phenotype and low total starch content (Figs 4, 5), implying that the *HvHGGT* mutation may also influence starch biosynthesis

during grain development. In comparison, the targeted mutation of *HvHPT* significantly reduced the content of both tocopherol and tocotrienol (Fig. 6). In *Arabidopsis*, a mutation to the *HPT* (*VTE2*) gene results in total tocopherol deficiency in seeds and seedlings, and the *vte2* mutants display severe seedling growth defects during germination (Sattler et al., 2004). As major lipid-soluble antioxidants in chloroplasts, tocopherols play specific functions in the plant redox-active pathway (Sattler et al., 2004). Additionally, tocopherol is required for the plant response to most abiotic stresses, such as high-intensity light stress (Havaux et al., 2005; Maeda and DellaPenna, 2007). In barley, the reduced tocopherol level in the *hpt* mutants may lead to a partially disrupted redox-active pathway and to tolerance to abiotic stresses, which might indirectly influence the accumulation of tocotrienol during grain development.

Because the knockout of *HvHPT* reduced the tocopherol content ~50 % compared to that of the wild-type grains (Fig. 6), *HvHPT* is partly responsible for tocopherol biosynthesis in barley, implying that potential *HvHPT* homologues or other genes might be involved in tocopherol production in barley. In oats, five different homologues/paralogues of the *HPT* gene were expressed and two of them were identified as highly correlated with tocopherol accumulation by deep sequencing and orthology-guided assembly (Gutierrez-Gonzalez et al., 2013; Gutierrez-Gonzalez and Garvin, 2016). Based on the barley genome database, a possible *HvHPT* homologue, *HORVU2Hr1G117600*, was found and it was specifically expressed in the barley grains (Supplementary Data Fig. S5). Transient overexpression of *HORVU2Hr1G117600* in tobacco leaves significantly increased the production of γ - and δ -tocopherol isoforms (Fig. S4), suggesting that *HORVU2Hr1G117600* may share the *HvHPT* function. This result may partly explain why the targeted mutation in *HvHPT* did not eliminate tocopherol production in barley grains.

Although *HORVU2Hr1G117600* was not expressed in leaves, tocopherol still accumulated in considerable amounts in the leaves of *hpt* mutants, suggesting that *HORVU2Hr1G117600* may not contribute to tocopherol biosynthesis in barley leaves. A recent study showed that many novel genes involved in fatty acid metabolism, chlorophyll metabolism and chloroplast function were potentially involved in the variation of tocopherol content in maize kernels (Wang et al., 2018). Interestingly, in a joint linkage and genome-wide association study of 5000 US maize lines revealed a lack of association between the *HPT* locus and tocopherol traits (Diepenbrock et al., 2017). In contrast, two novel large-effect loci (chlorophyll biosynthetic genes *por1* and *por2*) were identified as strongly correlated to tocopherol content in maize grains. These two genes encode homologues of protochlorophyllide reductase, which is involved in a highly regulated step in chlorophyll biosynthesis. Other studies have also noted that tocopherol biosynthesis is related to the chlorophyll biosynthesis pathway (Valentin et al., 2006; Zhang et al., 2015; Wang et al., 2018). Regarding the potential role of *HORVU2Hr1G117600* on tocopherol biosynthesis in grains but not in leaves, we propose that other non-tocopherol pathway-related genes might be involved in the accumulation of tocopherols in barley.

HGGT is predicted to be functionally divergent from HPT, which is conserved in both monocot and dicot species (Cahoon et al., 2003). Overexpression of monocot HGGT in *Arabidopsis* can functionally replace HPT in the biosynthesis

of vitamin E (Yang et al., 2011). However, we detected no *HvHGGT* expression in barley leaves, even though tocopherol was still synthesized in considerable amounts in *hpt* mutant lines (Supplementary Data Fig. S5). The results suggested that *HvHGGT* cannot replace the tocopherol biosynthesis function of *HvHPT* in barley. Our study functionally validated that *HvHGGT* is the only gene committed to produce tocotrienols, whereas *HvHPT* is partly responsible for tocopherol biosynthesis in barley. Hence, the vitamin E biosynthetic pathway has diverged between dicots and monocots, and the *HPT* homologue (*HORVU2Hr1G117600*) or other biosynthesis pathway-related genes may participate in the metabolic fluxes of tocopherol accumulation in barley and other monocots (Fig. 7). Therefore, this study expands our understanding of the vitamin E biosynthesis pathway in agronomically important cereal grains.

SUPPLEMENTARY DATA

Supplementary data are available online at <https://academic.oup.com/aob> and consist of the following. Figure S1: Comparison of amino acid sequences for barley genes. Figure S2: The trans-generational influence of Cas9 on the mutation type in T₁ transgenic barley plants. Figure S3: Phylogenetic relationship among the amino acid sequences of HPT and HGGT of barley and seven other plant species. Figure S4: Transient overexpression of *HORVU2Hr1G117600* in tobacco leaves by agro-infiltration. Figure S5: Semi-quantitative RT-PCR analysis of genes and the content of tocopherols in leaves and grains. Table S1: Primers used for making PTG editing constructs. Table S2: PTG sequences in the two editing constructs. Table S3: Primers for gene amplification. Table S4: Primers for semi-quantitative RT-PCR of genes. Table S5: Summary of results after barley genetic transformation. Table S6: The content of tocopherol isomers in *HvHPT* and *HvHGGT* T₂ grains of transgenic lines.

ACKNOWLEDGEMENTS

We thank Xinhang Jiang (College of Life Sciences, Zhejiang University, China) for his technical assistance with the HPLC analyses of tocopherols and tocotrienols of barley grains.

FUNDING

This work was supported by the National Natural Science Foundation of China (Grant Nos. 31971932 and 31771776), China Agriculture Research System (CARS-05-05A) and the Science Foundation of Zhejiang Province (Grant No. LGN18C130001).

LITERATURE CITED

- Aggarwal BB, Sundaram C, Prasad S, Kannappan R. 2010. Tocotrienols, the vitamin E of the 21st century: its potential against cancer and other chronic diseases. *Biochemical Pharmacology* **80**: 1613–1631.
- Andersson AAM, Lampi AM, Nystrom L, et al. 2008. Phytochemical and dietary fiber components in barley varieties in the HEALTHGRAIN diversity screen. *Journal of Agricultural and Food Chemistry* **56**: 9767–9776.

- Bramley PM, Elmadfa I, Kafatos A, et al. 2000.** Vitamin E. *Journal of the Science of Food and Agriculture* **80**: 913–938.
- Cahoon EB, Hall SE, Ripp KG, Ganzke TS, Hitz WD, Coughlan SJ. 2003.** Metabolic redesign of vitamin E biosynthesis in plants for tocotrienol production and increased antioxidant content. *Nature Biotechnology* **21**: 1082–1087.
- Cai S, Han Z, Huang Y, Hu H, Dai F, Zhang G. 2016.** Identification of quantitative trait loci for the phenolic acid contents and their association with agronomic traits in Tibetan wild barley. *Journal of Agricultural and Food Chemistry* **64**: 980–987.
- Chen J, Liu C, Shi B, et al. 2017.** Overexpression of *HvHGGT* enhances tocotrienol levels and antioxidant activity in barley. *Journal of Agricultural and Food Chemistry* **65**: 5181–5187.
- Chen S, Li H, Liu G. 2006.** Progress of vitamin E metabolic engineering in plants. *Transgenic Research* **15**: 655–665.
- Chin KY, Pang KL, Soelaiman IN. 2016.** Tocotrienol and its role in chronic diseases. *Advances in Experimental Medicine and Biology* **928**: 97–130.
- Collakova E, DellaPenna D. 2003.** Homogentisate phytyltransferase activity is limiting for tocopherol biosynthesis in *Arabidopsis*. *Plant Physiology* **131**: 632–642.
- Cui Y, Hu X, Liang G, et al. 2020.** Production of novel beneficial alleles of a rice yield-related QTL by CRISPR/Cas9. *Plant Biotechnology Journal* doi:10.1111/pbi.13370.
- DellaPenna D. 2005.** A decade of progress in understanding vitamin E synthesis in plants. *Journal of Plant Physiology* **162**: 729–737.
- Diepenbrock CH, Kandianis CB, Lipka AE, et al. 2017.** Novel loci underlie natural variation in vitamin E levels in maize grain. *The Plant Cell* **29**: 2374–2392.
- Falk J, Munne-Bosch S. 2010.** Tocochromanol functions in plants: antioxidation and beyond. *Journal of Experimental Botany* **61**: 1549–1566.
- Feng Z, Mao Y, Xu N, et al. 2014.** Multigeneration analysis reveals the inheritance, specificity, and patterns of CRISPR/Cas-induced gene modifications in *Arabidopsis*. *Proceedings of the National Academy of Sciences of the United States of America* **111**: 4632–4637.
- Gilliland LU, Magallanes-Lundback M, Hemming C, et al. 2006.** Genetic basis for natural variation in seed vitamin E levels in *Arabidopsis thaliana*. *Proceedings of the National Academy of Sciences of the United States of America* **103**: 18834–18841.
- Grebenstein N, Frank J. 2012.** Rapid baseline-separation of all eight tocopherols and tocotrienols by reversed-phase liquid-chromatography with a solid-core pentafluorophenyl column and their sensitive quantification in plasma and liver. *Journal of Chromatography A* **1243**: 39–46.
- Gutierrez-Gonzalez JJ, Garvin DF. 2016.** Subgenome-specific assembly of vitamin E biosynthesis genes and expression patterns during seed development provide insight into the evolution of oat genome. *Plant Biotechnology Journal* **14**: 2147–2157.
- Gutierrez-Gonzalez JJ, Tu ZJ, Garvin DF. 2013.** Analysis and annotation of the hexaploid oat seed transcriptome. *BMC Genomics* **14**: 471.
- Harwood WA. 2014.** A protocol for high-throughput *Agrobacterium*-mediated barley transformation. *Methods in Molecular Biology* **1099**: 251–260.
- Havaux M, Eymery F, Porfirova S, Rey P, Dörmann P. 2005.** Vitamin E protects against photoinhibition and photooxidative stress in *Arabidopsis thaliana*. *The Plant Cell* **17**: 3451–3469.
- Holme IB, Wendt T, Gil-Humanes J, et al. 2017.** Evaluation of the mature grain phytase candidate *HvPAPHy_a* gene in barley (*Hordeum vulgare* L.) using CRISPR/Cas9 and TALENs. *Plant Molecular Biology* **95**: 111–121.
- Horvath G, Wessjohann L, Bigirimana J, et al. 2006.** Accumulation of tocopherols and tocotrienols during seed development of grape (*Vitis vinifera* L. cv. Albert Lavallee). *Plant Physiology and Biochemistry* **44**: 724–731.
- Jones HD. 2015.** Regulatory uncertainty over genome editing. *Nature Plants* **1**: 14011.
- Kapusi E, Corcuera-Gómez M, Melnik S, Stoger E. 2017.** Heritable genomic fragment deletions and small indels in the putative ENGase gene induced by CRISPR/Cas9 in barley. *Frontiers in Plant Science* **8**: 540.
- Karunanandaa B, Qi Q, Hao M, et al. 2005.** Metabolically engineered oilseed crops with enhanced seed tocopherol. *Metabolic Engineering* **7**: 384–400.
- Keller Y, Bouvier F, d’Harlingue A, Camara B. 1998.** Metabolic compartmentation of plastid prenyllipid biosynthesis—evidence for the involvement of a multifunctional geranylgeranyl reductase. *European Journal of Biochemistry* **251**: 413–417.
- Kim YH, Lee YY, Kim YH, et al. 2011.** Antioxidant activity and inhibition of lipid peroxidation in germinating seeds of transgenic soybean expressing *OsHGGT*. *Journal of Agricultural and Food Chemistry* **59**: 584–591.
- Konda AR, Nazarene TJ, Nguyen H, et al. 2020.** Metabolic engineering of soybean seeds for enhanced vitamin E tocochromanol content and effects on oil antioxidant properties in polyunsaturated fatty acid-rich germplasm. *Metabolic Engineering* **57**: 63–73.
- Lawrenson T, Shorinola O, Stacey N, et al. 2015.** Induction of targeted, heritable mutations in barley and *Brassica oleracea* using RNA-guided Cas9 nuclease. *Genome Biology* **16**: 258.
- Lei Y, Lu L, Liu HY, Li S, Xing F, Chen LL. 2014.** CRISPR-P: a web tool for synthetic single-guide RNA design of CRISPR-system in plants. *Molecular Plant* **7**: 1494–1496.
- Li J, Meng X, Zong Y, et al. 2016.** Gene replacements and insertions in rice by intron targeting using CRISPR-Cas9. *Nature Plants* **2**: 16139.
- Liang Z, Chen K, Li T, et al. 2017.** Efficient DNA-free genome editing of bread wheat using CRISPR/Cas9 ribonucleoprotein complexes. *Nature Communications* **8**: 14261.
- Lushchak VI, Semchuk NM. 2012.** Tocopherol biosynthesis: chemistry, regulation and effects of environmental factors. *Acta Physiologiae Plantarum* **34**: 1607–1628.
- Maeda H, DellaPenna D. 2007.** Tocopherol functions in photosynthetic organisms. *Current Opinion in Plant Biology* **10**: 260–265.
- Maeda H, Sakuragi Y, Bryant DA, Dellapenna D. 2005.** Tocopherols protect *Synechocystis* sp. strain PCC 6803 from lipid peroxidation. *Plant Physiology* **138**: 1422–1435.
- Sattler SE, Gilliland LU, Magallanes-Lundback M, Pollard M, DellaPenna D. 2004.** Vitamin E is essential for seed longevity and for preventing lipid peroxidation during germination. *The Plant Cell* **16**: 1419–1432.
- Savidge B, Weiss JD, Wong YH, et al. 2002.** Isolation and characterization of homogentisate phytyltransferase genes from *Synechocystis* sp. PCC 6803 and *Arabidopsis*. *Plant Physiology* **129**: 321–332.
- Schneider C. 2005.** Chemistry and biology of vitamin E. *Molecular Nutrition & Food Research* **49**: 7–30.
- Sen CK, Khanna S, Roy S. 2007.** Tocotrienols in health and disease: the other half of the natural vitamin E family. *Molecular Aspects of Medicine* **28**: 692–728.
- Shen L, Wang C, Fu Y, et al. 2018.** QTL editing confers opposing yield performance in different rice varieties. *Journal of Integrative Plant Biology* **60**: 89–93.
- Valentin HE, Lincoln K, Moshiri F, et al. 2006.** The *Arabidopsis* vitamin E pathway gene5-1 mutant reveals a critical role for phytol kinase in seed tocopherol biosynthesis. *The Plant Cell* **18**: 212–224.
- Wang H, Xu S, Fan Y, et al. 2018.** Beyond pathways: genetic dissection of tocopherol content in maize kernels by combining linkage and association analyses. *Plant Biotechnology Journal* **16**: 1464–1475.
- Xie K, Minkenberg B, Yang Y. 2015.** Boosting CRISPR/Cas9 multiplex editing capability with the endogenous tRNA-processing system. *Proceedings of the National Academy of Sciences of the United States of America* **112**: 3570–3575.
- Yang Q, Zhong X, Li Q, et al. 2020.** Mutation of the D-hordein gene by RNA-guided Cas9 targeted editing reducing the grain size and changing grain compositions in barley. *Food Chemistry* **311**: 125892.
- Yang W, Cahoon RE, Hunter SC, et al. 2011.** Vitamin E biosynthesis: functional characterization of the monocot homogentisate geranylgeranyl transferase. *The Plant Journal: for Cell and Molecular Biology* **65**: 206–217.
- Zhang C, Zhang W, Ren G, et al. 2015.** Chlorophyll synthase under epigenetic surveillance is critical for vitamin E synthesis, and altered expression affects tocopherol levels in *Arabidopsis*. *Plant Physiology* **168**: 1503–1511.
- Zhang H, Zhang J, Wei P, et al. 2014.** The CRISPR/Cas9 system produces specific and homozygous targeted gene editing in rice in one generation. *Plant Biotechnology Journal* **12**: 797–807.